

The Liquid Phase of Superionic Conductors. MC Simulations of Molten Silver Iodide

C. Margheritis

Department of Inorg. Chemistry, University of Messina, Italy

Z. Naturforsch. **44a**, 567–572 (1989); received March 5, 1989

MC simulations, in the NpT version, were carried out on molten AgI, on the basis of the literature interionic potentials proposed for the simulation of the superionic α -phase of solid AgI. A systematic analysis showed that none of the examined potentials can satisfactorily reproduce the experimental characteristics of the melt.

Moreover, it has been pointed out that tests of pair potentials through simulations at constant volume can be misleading.

Key words: Interionic potentials, Monte Carlo simulation, Molten AgI.

Introduction

Superionic conductors show properties which are in between those of solids and liquids. They can be represented as two interpenetrating phases, the anions forming a stable sublattice through which the cations can move, thus behaving like a liquid.

Recently, the hypothesis has been formulated [1] that the superionic phases of solid conductors melt into very similar structures.

Although solid AgI, and especially the superionic phase α -AgI, has been extensively studied both experimentally and theoretically, very little work has been reported on the liquid phase [2].

Literature has given attention to the problem of correlating, by computer simulations, the properties of superionic α -AgI with appropriate potentials. Different sets of effective pair potentials were constructed and successively used in MD simulations.

In this work, the interionic potentials proposed for solid AgI are used in the simulation of molten AgI with the intention to evaluate simple thermodynamic and structural properties of the melt.

Solid AgI Pair Potentials

The first interionic potentials for solid AgI, given by Mayer [3] in 1933, have the form

$$\varphi_{ij}(r) = z_i z_j r^{-1} + a_{ij} \exp(-b_{ij} r) - c_{ij} r^{-6} - d_{ij} r^{-8}, \quad (1)$$

Reprint requests to Prof. C. Margheritis, Dipartimento di Chimica Fisica, Viale Taramelli 16, I-27100 Pavia, Italy.

where r is the distance between ions i and j having charge z_i, z_j while a_{ij}, b_{ij}, c_{ij} and d_{ij} are characteristic parameters. The second term in (1) is empirically determined from the constants of the crystal, while the last two terms are the van der Waals potential. According to Mayer, the constants in these latter quantities are large and should account for the low solubility, the high lattice energy and the zinc blende, preferred to rocksalt, lattice of this compound.

The numerical values for potential (1) are the following:

$$\begin{aligned} z_i z_j &= \pm e^2 \quad (e^2 = 2.30684 \cdot 10^{-18} \text{ J } \text{\AA} \text{ molecule}^{-1}), \\ b_{--} &= 2.90; \quad b_{+-} = 3.85; \quad b_{++} = 5.71 \text{ \AA}^{-1}, \\ a_{--} &= 270; \quad a_{+-} = 331; \quad a_{++} = 393 \\ &\quad \text{in } 10^{-17} \text{ J molecule}^{-1}, \\ c_{--} &= 437; \quad c_{+-} = 151; \quad c_{++} = 67 \\ &\quad \text{in } 10^{-19} \text{ J } \text{\AA}^6 \text{ molecule}^{-1}, \\ d_{--} &= 1228; \quad d_{+-} = 315; \quad d_{++} = 91 \\ &\quad \text{in } 10^{-19} \text{ J } \text{\AA}^8 \text{ molecule}^{-1}. \end{aligned}$$

More recently, Schommers [4] proposed an interionic potential consisting of only a Born-Mayer repulsive term and a Coulomb one. This potential, however, when used in MD simulations, requested each iodine to be attached to the lattice position by harmonic springs, in order to obtain a well defined iodine lattice.

In 1983, Parrinello, Rahman, and Vashishta [5] proposed a refined version of a previously calculated [6] set of potentials with constants determined from the physical characteristics of the low temperature structure.

0932-0784 / 89 / 0600-0567 \$ 01.30/0. – Please order a reprint rather than making your own copy.



Dieses Werk wurde im Jahr 2013 vom Verlag Zeitschrift für Naturforschung in Zusammenarbeit mit der Max-Planck-Gesellschaft zur Förderung der Wissenschaften e.V. digitalisiert und unter folgender Lizenz veröffentlicht: Creative Commons Namensnennung-Keine Bearbeitung 3.0 Deutschland Lizenz.

Zum 01.01.2015 ist eine Anpassung der Lizenzbedingungen (Entfall der Creative Commons Lizenzbedingung „Keine Bearbeitung“) beabsichtigt, um eine Nachnutzung auch im Rahmen zukünftiger wissenschaftlicher Nutzungsformen zu ermöglichen.

This work has been digitalized and published in 2013 by Verlag Zeitschrift für Naturforschung in cooperation with the Max Planck Society for the Advancement of Science under a Creative Commons Attribution-NoDerivs 3.0 Germany License.

On 01.01.2015 it is planned to change the License Conditions (the removal of the Creative Commons License condition “no derivative works”). This is to allow reuse in the area of future scientific usage.

Their interionic pair potential has the form

$$\phi_{ij}(r) = z_i z_j r^{-1} + A_{ij} r^{-n_{ij}} - B_{ij} r^{-4} - C_{ij} r^{-6}, \quad (2)$$

where the second term has the Pauling form of the repulsive potential while the third one should take into account the polarization energy [$B_{ij} = 0.5(\alpha_i z_j^2 + \alpha_j z_i^2)$]. On the basis of phonon dispersion measurements they assumed $|z_i| = |z_j| = 0.6e$. Thus, by using the polarizabilities $\alpha_{Ag} = 0$ and $\alpha_I = 6.52 \text{ \AA}^3$, the following numerical values (the distance being in \AA , the pair potential is in $10^{-19} \text{ J molecule}^{-1}$) were proposed:

$$\begin{aligned} n_{--} &= 7; & n_{+-} &= 9; & n_{++} &= 11; \\ A_{--} &= 10303.30; & A_{+-} &= 2640.87; & A_{++} &= 0.34; \\ B_{--} &= 54.15; & B_{+-} &= 27.07; & B_{++} &= 0; \\ C_{--} &= 159.94; & C_{+-} &= C_{++} = 0. \end{aligned}$$

This set of potentials was widely applied to the study of solid AgI and turned out to be very successful in describing, within MD simulations, structural and dynamical [7] properties along with phase transformations [8], in particular the temperature of the $\alpha \rightleftharpoons \beta$ transition. Recently, the partial structure factors of molten AgI were also calculated [1] at the experimental constant volume using the hypernetted chain approximation along with potentials (2).

Another set of potentials for solid AgI, largely applied in literature [9], was proposed in 1982 by Fukumoto, Ueda and Hiwatari [10], consisting of only a coulombic and a softcore repulsive term. The simplicity of this model allowed a systematic analysis [11] of the different forces for the existence of the α -phase, with the conclusion that weak Coulomb force is needed for the superionic phase to appear. According to these authors the set of potentials that, within simulations at constant volume, better describes the essential features of AgI, is the following:

$$\phi_{ij}(r) = z_i z_j r^{-1} + p_{ij} r^{-7} \quad (3)$$

with $|z_i| = |z_j| = 0.6e$ and $p_{--} = 4352.99$; $p_{+-} = 198.20$; $p_{++} = 0.69$ in $10^{-19} \text{ J \AA}^7 \text{ molecule}^{-1}$.

MC Simulations of Molten AgI

The above potentials were used in turn to carry out Monte Carlo simulations in the NpT version ($p = 1 \text{ atm}$), which allows a direct comparison with the experimental values. The model consisted of a cubic box containing 216 particles with periodic boundary conditions. The long-range Coulomb energy was

computed through the Ewald's sum (further details can be found in [12]).

When using potentials (3), equilibration of the system could not be reached. The system volume was constantly increasing up to $\approx 8000 \text{ cm}^3 \text{ mol}^{-1}$ after 700 kilosteps, thus denoting the lack of a cohesive force in respect to the repulsive one: it should be noted that, in the model assumed, the only cohesive force is the $+-$ coulombic term.

In order to reach the equilibration of the system, test runs were carried out with different parameters, within the same potential model. In particular attention was focused on the $--$ term, for which a drastic reduction seemed necessary. When p_{--} was decreased by an order of magnitude (i.e. $p_{--} = 435.3 \cdot 10^{-19} \text{ J \AA}^7$) the simulated system could be equilibrated, but the calculated volume was still too large ($V_m = 144 \text{ cm}^3 \text{ mol}^{-1}$ at the m.p.).

Thus, only potentials (1) and (2) were employed for further analysis.

Thermodynamic Properties

The AgI melt was analyzed at three different temperatures (831 (m.p.), 1000 and 1500 K). The results are summarized in Table 1. The experimental values of the molar volumes, V_m , shown in the first row, were deduced from the density data reported by Janz et al. [13] for the temperature range 840–1080 K. For what concerns the internal energy, U , the experimental data were calculated on the basis of the -208.0 kcal/mole value given for α -AgI at 523 K by Flengas [14], along with the $C_p(\alpha\text{-AgI})$ by [15], the $C_p(\text{melt})$ by [16] and the ΔH_f reported in [17]. Different literature values are of the same order of magnitude (e.g. at 298 K the experimental value given by Mayer [3] is -196.2 and that by Tosi [18] is $-208.1 \text{ kcal/mole}^{-1}$). It should be noted that, since silver iodide is not purely ionic, these experimental data, based on a Born-Haber cycle, can be in error.

Columns B of Table 1 report the values obtained by potential (1), in connection with the SIM model (briefly: the polarization energy of the system is also taken into account within the MC cycle as a many body interaction [19]). As it can be noted, the molar volumes are fairly well reproduced by Mayer's potential, the experimental values lying in between those obtained with potentials (1) used without or with the contribution of the polarization energy. On the con-

Table 1. Molar volumes and energies for molten AgI (in $\text{cm}^3 \text{mol}^{-1}$ and kcal mol^{-1} respectively) obtained with: A=potential (1); B=potential (1) within the SIM model; C=potential (2).

	831 K (m.p.)			1000 K			1500 K		
$V_m(\text{exp})$	42.1			43.4			47.9*		
$-U(\text{exp})$	201.5			198.9			191.3		
Potential type	A	B	C	A	B	C	A	B	C
V_m	42.0	40.3	57.5	44.6	42.0	61.1	55.3	48.3	80.2
$-U$	166.5	171.0	69.2	163.2	168.4	66.9	153.7	162.3	58.6
$-E^C$	184.8	187.5	62.6	182.4	185.4	61.6	175.4	181.5	58.1
E^R	43.3	47.7	26.0	41.6	46.7	24.7	36.7	45.1	19.8
$-E^W$	30.0	32.1	1.1	28.4	30.9	1.1	23.9	28.2	0.8
$-E^{-4}$	—	—	36.5	—	—	34.9	—	—	28.4
$-E^P$	—	4.1	—	—	4.8	—	—	6.6	—

* Extrapolated value.

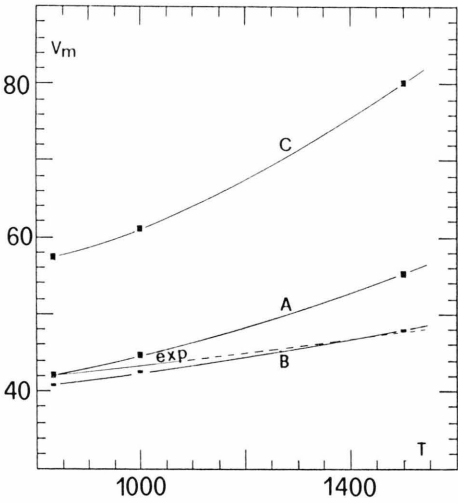


Fig. 1. Molar volumes ($\text{cm}^3 \text{mol}^{-1}$) calculated at different temperatures (T/K) according to potential (1) (curve A), potential (1) with the SIM model (curve B) and potential (2) (curve C). The experimental curve is also given.

trary, the system simulated by potentials (2) is significantly expanded. Figure 1 illustrates these results. Note also that no one of the calculated functions has the proper temperature dependence.

As regards the internal energies, all the calculated values are far from those obtained by the Born-Haber cycle. Moreover, the average C_p values that can be deduced are ≈ 19 , 14 and 15 ($\text{cal K}^{-1} \text{mol}^{-1}$) for model A, B and C respectively, which should be compared with the experimental value of 15.26 ($\text{cal K}^{-1} \text{mol}^{-1}$). Table 1 also reports the values obtained for the Coulomb, E^C , van der Waals, E^W , repulsive, E^R , along with the r^{-4} , E^{-4} , components of the average configurational energy. Energies U and E are

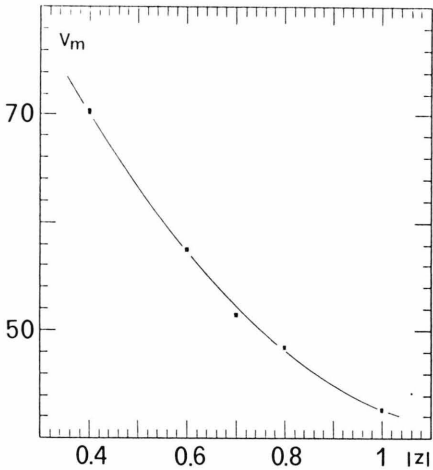


Fig. 2. Molar volumes ($\text{cm}^3 \text{mol}^{-1}$) calculated at 831 K with potential (2) with different ionic charges.

related by $U = E + 3RT$. In addition, the polarization component, E^P , calculated in connection with the SIM model of potential (1), is reported.

In order to complete the analysis, attempts were made to specify the effects of some parameters. Thus, potentials (2) were used first with different ionic charges, namely $|z_i| = 0.4, 0.7, 0.8$ and 1 e and then at constant volume ($V = V_{\text{exp}}$) with $|z_i| = 0.6\text{ e}$. The results obtained at 831 K are summarized in Table 2. As can be noted, the imposition of the constant volume does not significantly change the energy values, while the ionic charge largely affects both the volume and the energy. It is interesting to observe that in order to obtain V_m values close to the experimental ones the

Table 2. Molar volumes and energies (in $\text{cm}^3 \text{mol}^{-1}$ and kcal mol^{-1} , respectively) calculated according to potential (2) with variable ionic charge (0.4, 0.7, 0.8 and 1 e in columns C04, C07, C08 and C1, respectively) and at constant volume (CV) at $T = 831 \text{ K}$.

	C04	C07	C08	C1	CV
V_{calc}	70.3	51.4	48.4	42.6	—
$-U_{\text{calc}}$	32.4	94.1	123.3	195.9	70.7
$-E^{\text{C}}$	25.3	88.4	119.4	197.0	65.7
E^{R}	17.0	31.9	37.7	51.8	40.1
$-E^{\text{W}}$	0.8	1.4	1.5	2.0	1.9
$-E^{-4}$	28.3	41.2	45.1	53.7	48.2

ionic charge has to be raised to 1. Figure 2 clearly shows the effect of the ionic charge on the molar volume.

Structural Properties

The experimental structure parameters (both partial structural factors and radial distribution functions) for solid AgI have been extensively studied using X-ray [20] and neutron [21] diffraction and are fairly well reproduced either by potentials (2) [5, 6, 7, 22] or by (3) [10, 11]. The analogous data for molten AgI have not yet been reported.

Nevertheless the results by Howe and McGreevy [21] are consistent with the hypothesis that the silver–silver distribution in α -AgI is similar to that of copper ions in molten cuprous chloride. Thus one would expect for molten AgI a structure that closely resembles that of molten CuCl, which [23] shows a I–I radial distribution function, $g_{\text{II}}(r)$, characterized by a rather far ranging oscillatory pattern, while $g_{\text{CuCu}}(r)$ is much less structured, with copper ions penetrating deeply into the first coordination shell.

A neutron diffraction study carried out on molten AgI by M. A. Howe and R. L. McGreevy [24] shows a relatively long range I structure (up to 14 \AA); this appears very different from the Ag structure which hardly shows any oscillation beyond 8 \AA . The positions of the maxima in the two functions are also very different. The simulation results are reported in Figure 3, where the three radial distribution functions, $g_{\text{AgI}}(r)$, $g_{\text{AgAg}}(r)$ and $g_{\text{II}}(r)$ obtained with potentials (1) and (2) at 831 K are shown.

As it can be noted, the $g(r)$ of like ions obtained with potentials (1) are not much different. On the contrary, those obtained with potentials (2) closely resemble the molten CuCl structure.

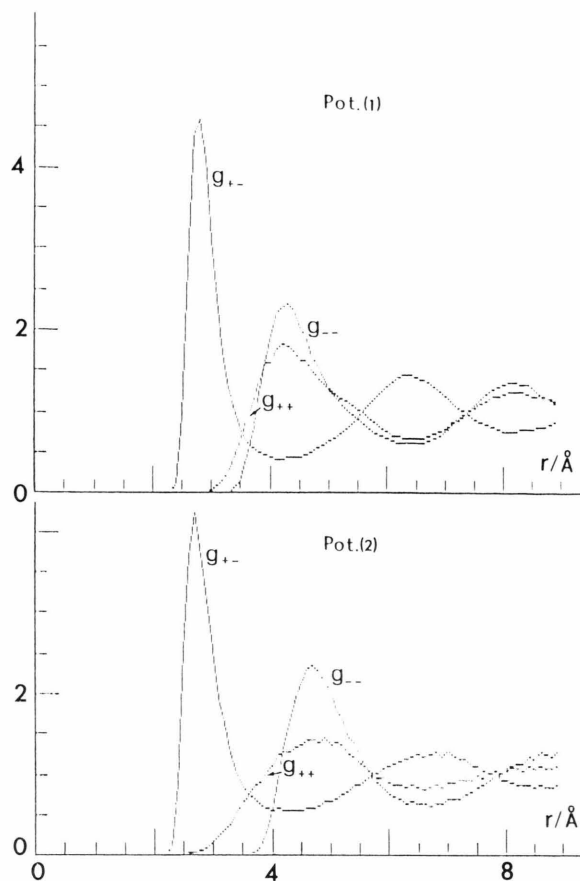


Fig. 3. Radial distribution functions for molten AgI obtained at 831 K with potentials (1) and (2).

The effect on the $g(r)$'s of different values of the ionic charge was also analyzed. Figure 4, which reports the functions obtained with $|z_i| = 0.4, 0.8$ and 1 e , shows that with decreasing charge: a) the peaks are lowered and shifted to the right; b) the oscillatory pattern decreases, the melt being less structured; c) the silver penetration into the first coordination shell increases. It should be noted that with decreasing charge the volume of the simulated system increases and its effect should also be taken into account, but it is anyhow overwhelmed by that of the charge.

The $g(r)$'s obtained while imposing the experimental volume show that this constraint largely affects the $g_{\text{II}}(r)$: the distance of closest approach is reduced and the position of the first maximum, along with that of the following minimum, is reduced by $\approx 0.7 \text{ \AA}$. The $g_{\text{AgAg}}(r)$ is also affected, though to a smaller extent; on the contrary, the $g_{\text{AgI}}(r)$ remains practically the same.

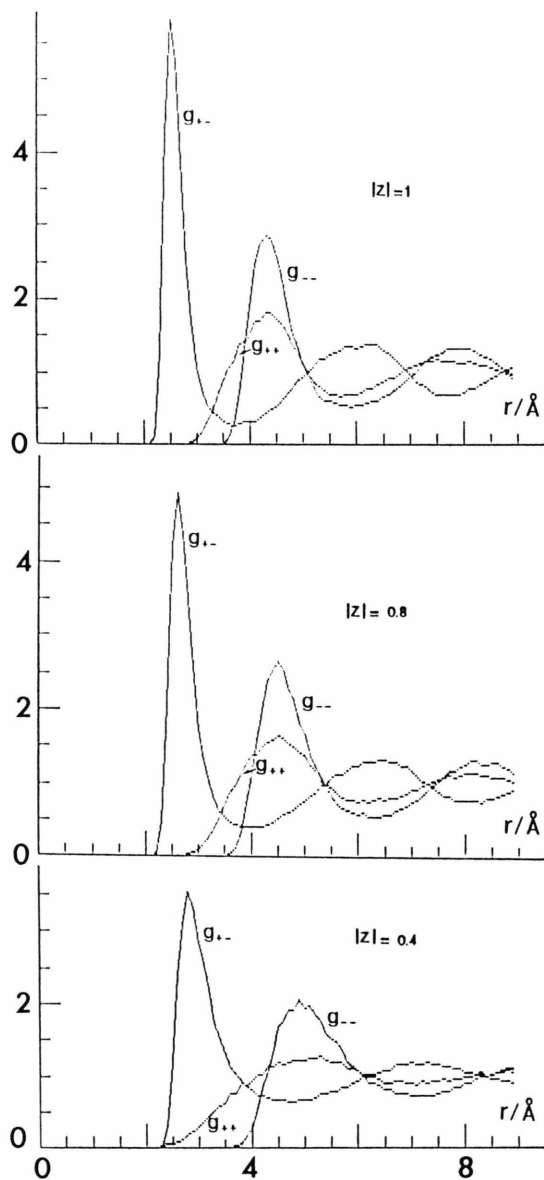


Fig. 4. Radial distribution functions for molten AgI at 831 K calculated according to potentials (2) with different ionic charges.

Finally Table 3 reports the distance of closest approach, d , the position of the first maximum (r_{\max}) and that of the following minimum (r_{\min}), along with the coordination number (n), calculated using potentials (1), (2) and (2) at constant volume. In order to avoid redundancy, the parameters of the total $g(r)$'s are not reported; however, it is interesting to observe that

Table 3. Main features of the radial distribution functions calculated for molten AgI at 831 K using potentials (1), (2) and (2) at constant volume (CV) (distances in Å).

Potential type		(1)	(2)	(CV)
$\text{Ag}^+ - \text{Ag}^+$ pairs	d	2.7	2.2	2.1
	r_{\max}	4.2	4.9	4.4
	r_{\min}	6.6	6.6	6.3
	n	16.0	12.0	14.3
$\text{Ag}^+ - \text{I}^-$ pairs	d	2.3	2.2	2.2
	r_{\max}	2.8	2.7	2.6
	r_{\min}	4.1	4.3	4.2
	n	4.9	3.9	4.9
$\text{I}^- - \text{I}^-$ pairs	d	3.2	3.5	3.4
	r_{\max}	4.3	4.7	4.3
	r_{\min}	6.4	6.7	6.2
	n	14.8	12.7	13.7

these functions show a minimum at 3.5, 3.7, 3.6 Å, respectively, and the corresponding coordination numbers are 4.2 (of which 4.1 + − and 0.1 + +), 3.5 (3.2 + − and 0.3 + +), and 4.3 (3.9 + − and 0.4 + +). These figures once again underline that only potentials (2) can reproduce a significant penetration of silver ions into the first coordination shell.

Conclusions

On the basis of these results, one must conclude that none of the examined potentials, designed for the solid AgI, can satisfactorily reproduce the experimental characteristics of the melt. In particular the potentials (2), that have so successfully been applied to reproduce structural and dynamical properties of α -AgI, fail in reproducing even approximately the volume of the melt. On the contrary, Mayer's potentials reproduce the density well, but seem to fail in reproducing the structure of the melt.

It is hoped that, once the experimental $g(r)$'s will be available, it will be possible to properly modify the potentials and thus to obtain a satisfactory simulation of the melt.

Moreover, attention should be given to the problem of testing pair potentials through simulations at constant volume, as in MD, since this could be misleading, as the use of potentials (3) within the NpT MC clearly shows.

Acknowledgement

This work was partially supported by a CNR grant.

- [1] A. J. Stafford and M. Silbert, *Z. Phys. B – Condensed Matter* **67**, 31 (1987).
- [2] P. Vashishta, J. N. Mundy, and G. K. Shenoy (eds.), *Fast Ion Transport in Solids*, North Holland, New York 1979, p. 507.
- [3] J. E. Mayer, *J. Chem. Phys.* **1**, 327 (1933).
- [4] W. Schommers, *Phys. Rev. Lett.* **38**, 1536 (1977).
- [5] M. Parrinello, A. Rahman, and P. Vashishta, *Phys. Rev. Lett.* **50**, 1073 (1983).
- [6] P. Vashishta and A. Rahman, *Phys. Rev. Lett.* **40**, 1337 (1978).
- [7] See e.g.: a) P. Vashishta, *Solid State Ionics* **18**, **19**, 3 (1986). – b) G. L. Chiarotti, G. Jacucci, and A. Rahman, *Phys. Rev. Lett.* **57**, 2395 (1986).
- [8] J. Tallon, *Phys. Rev. Lett.* **57**, 2427 (1986).
- [9] See e.g.: a) M. Hokazono, A. Ueda, and Y. Hiwatari, *Solid State Ionics* **13**, 151 (1984). – b) Y. Kaneko and A. Ueda, *J. Phys. Soc. Japan* **55**, 3924 (1986).
- [10] A. Fukumoto, A. Ueda, and Y. Hiwatari, *J. Phys. Soc. Japan* **51**, 3966 (1982).
- [11] Y. Kaneko, A. Ueda, and Y. Hiwatari, *J. Phys. Soc. Japan* **55**, 1244 (1986).
- [12] See e.g.: C. Margheritis and C. Sinistri, *Z. Naturforsch.* **30a**, 83 (1975).
- [13] Janz et al., *Natl. Std. Ref. Data Ser. Natl. Bur. Std. (USA)*, Nr. 15, p. 81 (1968).
- [14] S. N. Flengas and E. Rideal, *Proc. Roy. Soc. A* **233**, 443 (1956).
- [15] J. Nolting and D. Rein, *Z. Physik. Chem.* **66**, 150 (1969).
- [16] *Gmelins Handbuch der anorganischen Chemie*, 8. Aufl., Silber, Teil B2, p. 249 (1972).
- [17] C. E. Wicks and F. E. Block, *U.S. Bur. Mines Bull.* **605**, 107 (1963).
- [18] M. P. Tosi, in: *Solid State Physics*, Academic Press, New York 1964, Vol. 16, p. 64.
- [19] C. Margheritis and C. Sinistri, *Z. Naturforsch.* **43a**, 129 (1988).
- [20] T. M. Hayes and J. B. Boyce, *J. Phys. C: Solid State Phys.* **13**, L731 (1980).
- [21] M. A. Howe, R. L. McGreevy, and E. W. J. Mitchell, *Z. Phys. B – Condensed Matter* **62**, 15 (1985).
- [22] H. Okazaki and F. Tachibana, *Solid State Ionics* **9**, **10**, 1427 (1983).
- [23] S. Eisenberg, J. F. Jal, and J. Dupuy, *Phil. Mag. A* **46**, 195 (1982).
- [24] Private communication, which the author gratefully acknowledges.